J. Sci. Math. Res. (2026) Vol. 6, pp. 1-14 Published by Centaurus Press
(Received 2026-06-09)

Helical vortex rings in the wake of a disk

Thad S. Morton

The structure of the wake behind a circular disk is examined in numerical solutions for $Re = 50$, 100, and 120. A slowly reversing helical (swirling) vortex was found to exist in the steady numerical solutions at these flow speeds, which are generally regarded as steady and axisymmetric. The nested stream surfaces resemble Reeb foliations. The loss in fore/aft symmetry of the pressure field due to the viscous term may be associated with the azimuthal drift seen in the streamlines.

1. Introduction

Suppose you are a fluid particle trapped in the wake vortex trailing a circular disk held normal to a uniform flow. How many times could you expect to loop around in the vortex before being finally released into the downstream field? If the answer is, say, 100 times, would you expect to travel the exact same loop 100 times? If your paths were exactly the same all 100 times, what would change on the 101st time around that would allow you to finally exit? If the flow is strictly axisymmetric, then whatever this change is, it cannot occur in the azimuthal direction. If the spherical vortex of Hill (1894) is any indication of the behaviour of the flow, the viscous influence on the pressure field might bear some of the responsibility for almost imperceptible swirl arises in flows regarded as axisymmetric.

As with the wake of a sphere and a cube, there is a critical Reynolds number for flow past a normal disk, above which swirl appears, and the wake vortex takes on an asymmetric form while remaining steady. The critical Reynolds number above which axisymmetry in a disk wake is lost is denoted Re_{C1}. After this critical Reynolds number is exceeded, the flow remains steady until a second critical Reynolds number, Re_{C2}, is exceeded and the flow becomes unsteady. Fernandes *et al.* (2007) reported that for flow normal to a disk, these critical Reynolds numbers are given by

$$Re_{\mathrm{C1}} = 116.5(1+\chi^{-1}) \qquad \text{(loss of axisymmetry)} \qquad (1)$$

$$Re_{\mathrm{C2}} = 125.6(1+\chi^{-1}), \qquad \text{(loss of steady flow)} \qquad (2)$$

where $\chi = D/t$ is the ratio of the cylinder diameter to the cylinder height (or disk diameter to disk thickness).

Marshall & Stanton (1931) reported that the onset of unsteadiness in the wake of a disk with $\chi = 10$ occurred at $Re \approx 195$ (see also Stanton and Marshall 1932), which is delayed somewhat according to (1) and (2).

Magarvey and Bishop (1961) found that when Reynolds number for flow past a sphere exceeds approximately 200, the wake bubble undergoes a distortion into an asymmetrical shape so that an entirely different quasi-steady flow field results. Clear depictions of this phenomenon are shown by Johnson and Patel (1999) for the sphere and Saha (2004) for the cube. Johnson and Patel verified the findings of Magarvey and Bishop and found that for the sphere, $Re_{\mathrm{C1}} = 210$ and $Re_{\mathrm{C2}} = 290$. Saha (2004) found that for flow past a cube, Re_{C1} was between 216 and 218 and Re_{C2} was between 265 and 270.

Natarajan and Acrivos (1993) analyzed the axisymmetric steady Navier–Stokes solution for flow past a normal circular disk and found a linear instability of the axisymmetric steady base flow (the real part of the eigenvalue became positive) at $Re_1 = 58.25$, meaning that at this Reynolds number, the axisymmetric steady solution becomes unstable to a steady 3D/asymmetric mode. They also followed that branch and found a second complex eigenvalue crossing into the right half-plane; however, once the Reynolds number exceeds Re_1, the axisymmetric base flow is no longer physically realized. The system instead moves onto a new asymmetric steady branch, so their second critical value of $Re_2 = 62.8$ is not as physically relevant (Fabre, Auguste, and Magnaudet 2008).

The numerical solution of Shenoy and Kleinstreuer (2008) for flow past a circular disk with $\chi = 10$ showed steady, axisymmetric flow for $(10 < Re < 135)$, and unsteady, asymmetric flow structure for $Re > 135$, in agreement with (1) and (2).

Yang *et al.* (2014) found for $\chi = 5$ the first bifurcation at $Re_1 = 120$, leading to the steady state mode with a reflectional symmetry and a double-thread wake extending to the downstream. They found a Hopf bifurcation at $Re = 152$, at which planar symmetry was lost, and a third bifurcation at $Re = 166$.

At higher speeds (in the range $1.5\times10^4 \le Re \le 3\times10^5$), Berger *et al.* (1990) found three frequencies in a disk wake: one at a very low Strouhal number of $S_1 = f_1 D/v_\infty = 0.05$ due to an axisymmetric pulsation of the recirculation bubble, one at $S_n = 0.135$ associated with "antisymmetric" fluctuations induced by a helical vortex structure, and a higher frequency instability at $S_3 = 12\,S_n$. By "antisymmetric," Berger *et al.* were referring to a frequency alternating across the central axis of symmetry at, or about, 180° apart. From the magnitude of their reported S_n, it was almost certainly due to the primary vortex shedding, which can be approximated conceptually by $S_n \approx n/(2\pi)$, where n is the number of vortices shed per shedding cycle (Morton 2007, Levi 1983). For axisymmetric flow, $n = 1$, and for planar flow, $n = 2$. Tian *et al.* (2016) obtained $S_1 = 0.01$, $S_n = 0.148$, and $S_3 \approx 0.8$-1.35, and showed probably the clearest view and most quantitative description of the mean wake bubble trailing the normal disk with $\chi = 50$, including velocity profiles and kinetic energy profiles.

Table 1 shows Strouhal numbers found for flow past circular disks at various Reynolds numbers. Studies of falling disks are not included in the table.

χ	**Study**	Re	St_1	St_n	St_3	**Source**
5	LES	152, 172		0.1132	$2\,St_n$	Yang *et al.* (2014)
10	DNS	160, 180		0.113	$2\,St_n$	Shenoy & Kleinstreuer (2008)
3	DNS	179.8		0.109		Auguste *et al.* (2010)
~10	Experiment	191		0.128		Marshall & Stanton (1931)
~10	Experiment	197		0.121		Marshall & Stanton (1931)
~10	Experiment	199		0.124		Marshall & Stanton (1931)
~10	Experiment	200		0.117		Marshall & Stanton (1931)
5	LES	270	0.035	0.1355	$2\,St_n$	Yang *et al.* (2014)
10	DNS	300	0.041	0.122	$2\,St_n$	Shenoy & Kleinstreuer (2008)
	Experiment	1.58×10^4		0.14		Hwang & Baldwin (1966)
32	Experiment	3.5×10^4 ~ 5×10^4		0.136		Calvert (1967)
~10	Experiment	5×10^4		0.14	$2St_n$	Fuchs *et al.* (1979)
10, 14	Experiment	$10^4 \sim 10^5$		0.135~0.149 (linear)		Miau *et al.* (1997)
	Experiment	1.9×10^4		0.135		Hwang & Baldwin (1996)
	Experiment	7.8×10^4		0.135		Roberts (1973)
50	Experiment	1.4×10^5		0.138		Lee & Bearman (1992)
50	LES	1.5×10^5	0.01	0.148		Tian *et al.* (2016)
43	Experiment	1.4×10^5	0.05	0.135	$12\,S_n$	Berger *et al.* (1990)
67	Experiment	1.9×10^5	0.05	0.135	$12\,S_n$	Berger *et al.* (1990)
67	Experiment	2.5×10^5	0.05	0.135	$12\,S_n$	Berger *et al.* (1990)

Table 1. Strouhal numbers for normal disks at various Reynolds numbers.

2. Solution Grid

A section of the 3-D mesh generated using automatic mesh refinement in SolidWorks Flow Simulation is shown in Figure 1 and Figure 2.

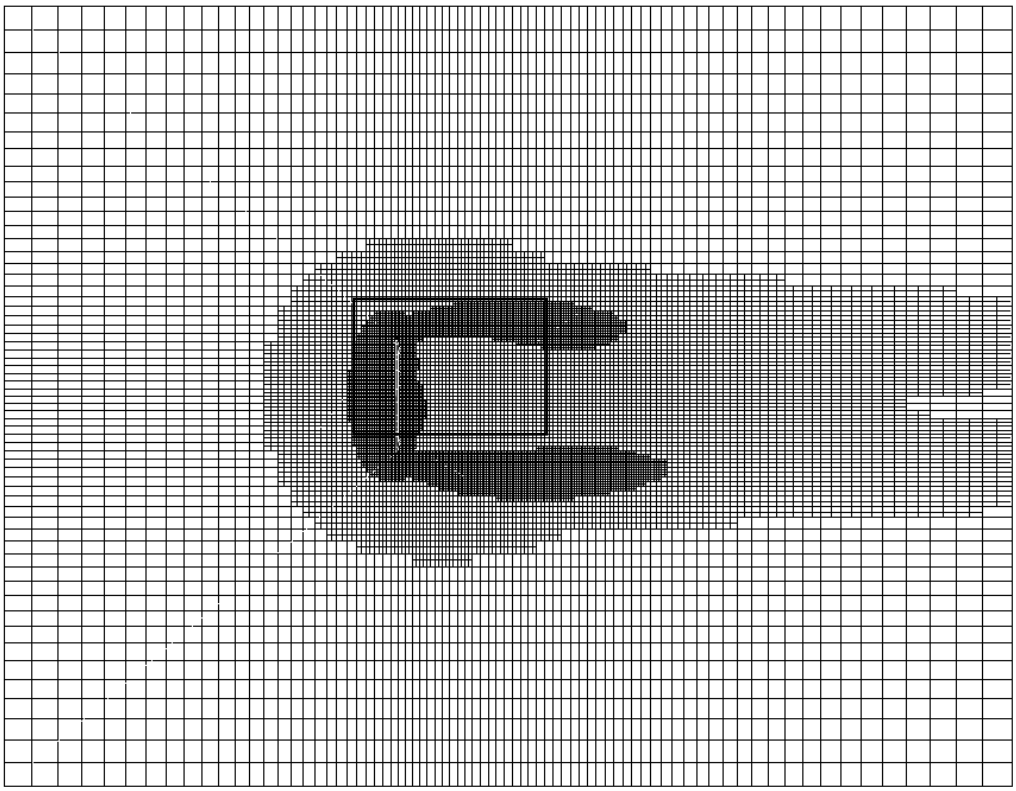

Figure 1. Section from the computational grid used for flow normal to a disk using SolidWorks Flow Simulations' automatic 3-D mesh refinement.

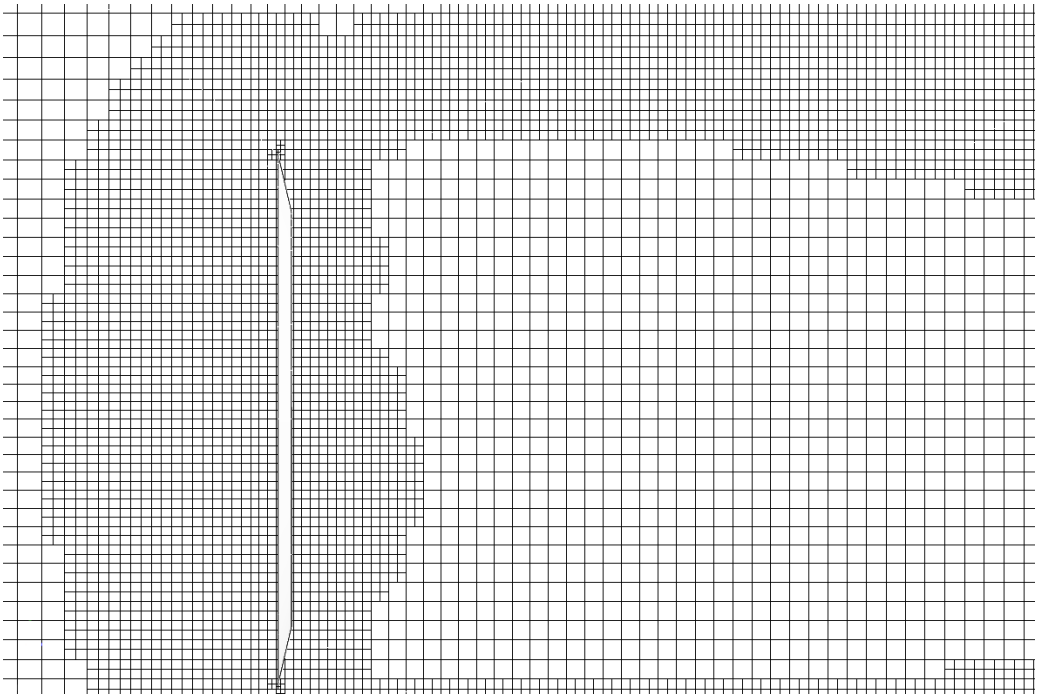

Figure 2. Close-up view of Figure 1. Number of computational cells: 619,366. $Re = 120$.

3. Results

In the present study, steady numerical solutions were obtained for flow normal to a sharp-edged circular disk for $Re = 50$, 100, and 120 (with Reynolds number based on disk diameter of $D = 0.1$ m) using commercially available SolidWorks Flow Simulation software. The drag coefficients for all cases of the present study are shown plotted in Figure 3 along with the measurements of Willmarth *et al.* (1964) and Roos and Willmarth (1971), and the numerical simulations of Nitin and Chhabra (2005) and Mishra *et al.* (2019).

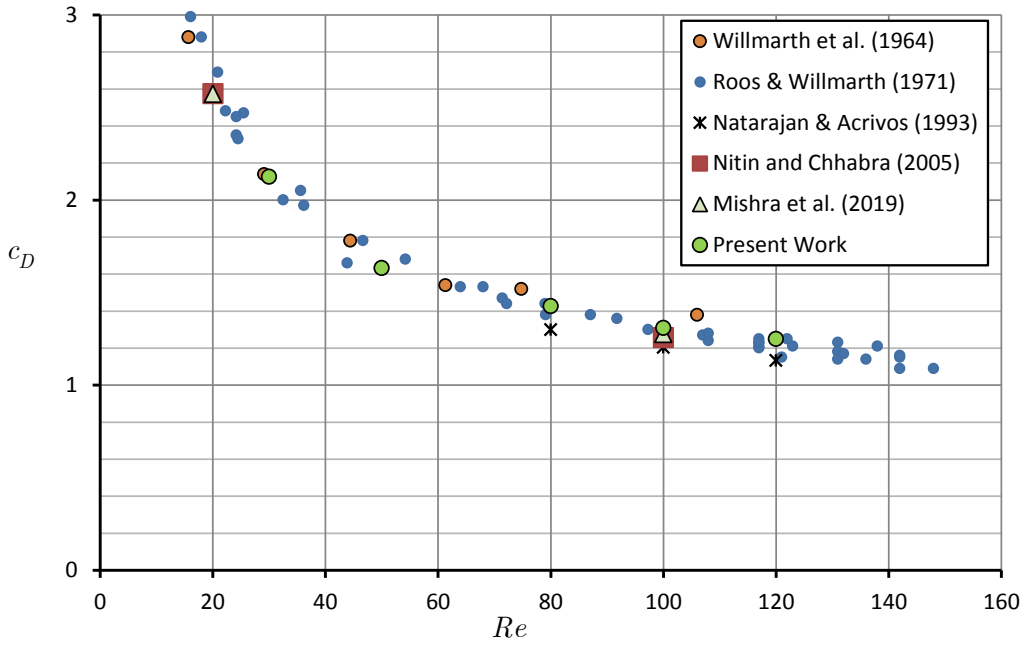

Figure 3. Drag coefficient of a disk normal to the flow.

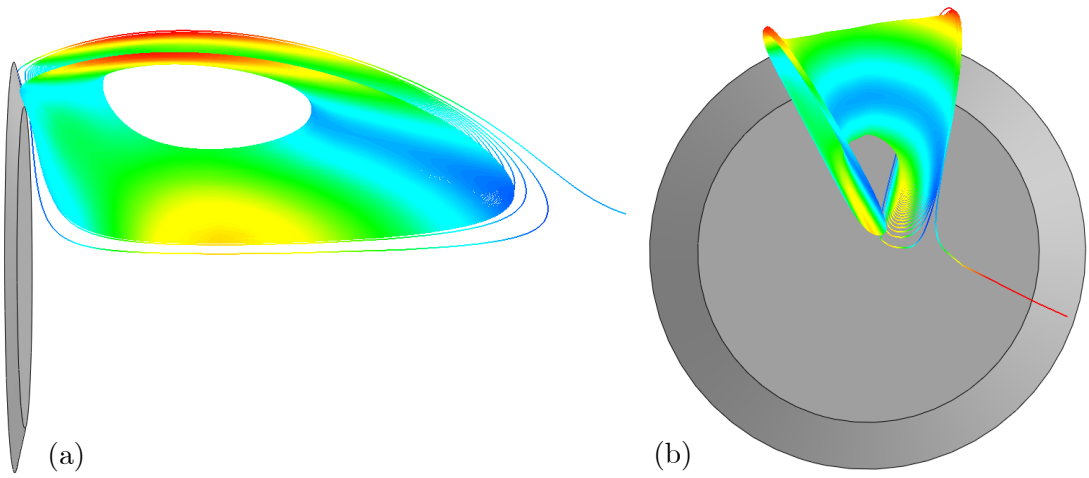

Figure 4. Wake vortex behind a circular disk at $Re = 50$ showing weak swirl in the azimuthal direction. The color scales of all streamlines represent velocity magnitude. (a) Side view. (b) Rear view. Number of computational cells: 1,897,313. $c_D = 1.63$.

It was found that steady helical structures arise in the wake of the circular disk at Reynolds numbers as low as 50. Results for flow past a disk at $Re = 50$ shown in Figure 4 indicate a gradual swirl developing in the azimuthal direction, as do the results for $Re = 100$ shown in Figure 5.

Even for the flows that are steady and below the first critical Reynolds number where axisymmetry holds, if a single streamline is tracked for long time, the steady solution shows that the streamline creates a very gradual foliation, or azimuthal drift, within the toroidal vortex in the disk's wake bubble. The slight deviation from axisymmetry due to very gradual swirl in the wake bubble trailing the disk appears to begin at Reynolds numbers as low as 45.

In the solutions of this study, there is no vortex shedding, so the flows could be construed as steady. If the wake were sectioned through the symmetry axis, the view would be indistinguishable from an axisymmetric flow. In fact, this flow may have cyclic symmetry about the axis because the swirl pattern is repeated at other angles around the axis.

The flow at $Re = 100$ in Figure 6 shows a slowly reversing helix. The azimuthal migration of the flow is so gradual that a section containing the axis will not reveal it. Figure 6 shows foliations within the toroidal flow. These resemble Reeb foliations (Reeb 1952; see Lawson 1974 p. 378; Candel and Conlon 2000 Chapter 5), but Reeb foliations spiral continually outward and bunch up near the outer boundary of the torus (Bachman 2012, p. 80). The foliations in the wake of the circular disk, on the other hand, reverse course near the outer boundary. However, a shape similar to the trumpet shape seen on the right side in Figure 6 is depicted for a Reeb foliation by Camacho and Neto (1984, p. 45).

The gradual azimuthal drift of the streamlines seen in Figure 5 and Figure 6 are reminiscent of the "Yin-Yang" wake pattern mentioned in the landmark study by Auguste *et al.* (2010) in connection with their flow at $Re = 195$.

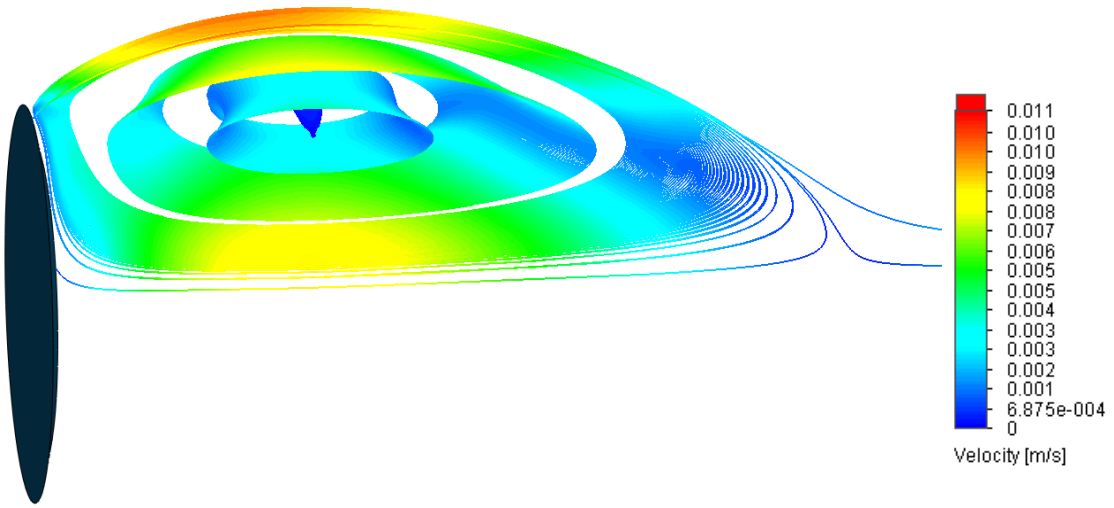

Figure 5. Wake vortex behind a circular disk at $Re = 100$ showing weak swirl in the azimuthal direction. Four of the six streamlines have begun slowly tracing out vortex tubes. Number of computational cells: 604,190. $\nu = 1.818 \times 10^{-5}\,\mathrm{m}^2/\mathrm{s}$, $c_D = 1.307$.

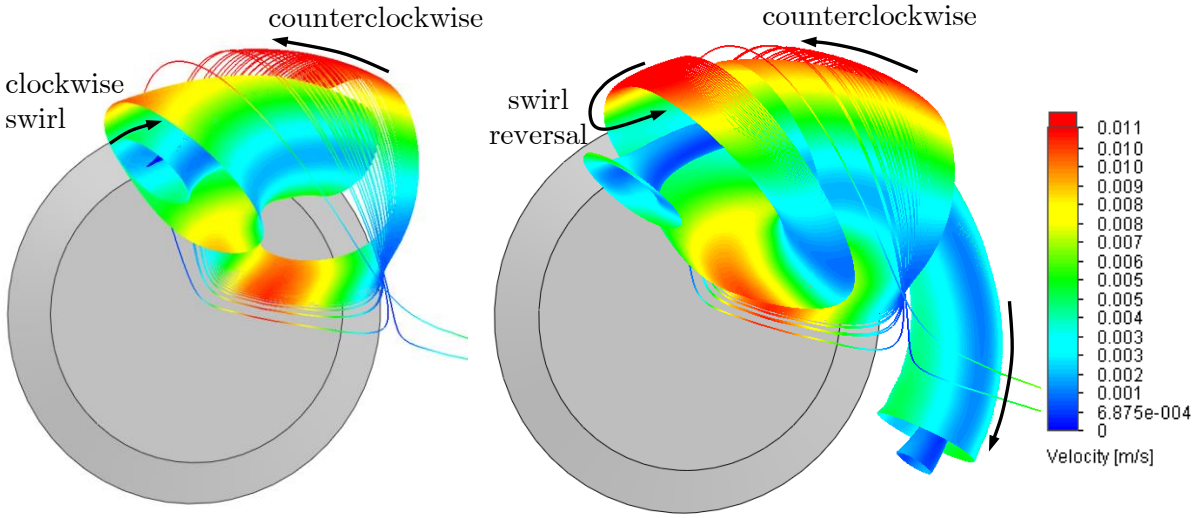

Figure 6. Steady numerical solution of the flow behind a circular disk at $Re = 100$. The swirl exhibits a slow reversal from counterclockwise on the outside to clockwise near the core circle. $\nu = 1.818 \times 10^{-5}\,\mathrm{m}^2/\mathrm{s}$, $c_D = 1.307$.

Figure 7(a) and (c) show a single streamline in the wake of a circular disk at $Re = 120$. The diameter-to-thickness ratio in the present study was $\chi = 40$. According to the formula in (1), $Re_{\mathrm{C1}} = 119$ (or less, since the disk thickness even decreased to a sharp edge), and using $\chi = 40$ in (2) yields $Re_{\mathrm{C2}} = 128.6$. So the flow observed in the present study agrees with the findings of Fernandes *et al.* (2007)—the flow at $Re = 120$ was steady but asymmetric.

The angled plane approximately sketched out by the streamline in Figure 7 appears to divide the wake bubble in half, with streamlines appearing on one side of it remaining trapped on that side. This is shown in Figure 7(b), wherein a second streamline remains entirely confined to the left side of the plane. Figure 7(c) and (d) show side views of the flows in Figure 7(a) and (b), respectively.

Jeffreys (1930) conjectured that "A single helical vortex is not a possible wake" because of the circulation theorem. In a study of the near wake behind spheres and disks, Berger *et al.* (1990) noted that, contrary to Jeffreys' conjecture, helical vortices can, in fact, exist and that the circulation theorem can be seriously violated by turbulent diffusion.

Although Jeffreys (1930) concluded that "it appears… that the wake cannot consist of a helical vortex or a combination of two helical vortices," the following remarks by him, while made in connection with the von Kármán vortex street, are interesting in the present context in light of the swirl reversals found here in the wake of a disk: "The alternative mechanism seems to be that the whole of the vorticity passes down the helix, but turns round and comes back along the axis… There are two possible ways of combining helical vortices so as to keep the circulation zero about a circle drawn in the fluid that has not been near the solid. Two helices may be wound on the same cylinder. If they twist in opposite senses, they intersect twice in each turn about the axis of the helix… If they twist in the same sense and do not intersect, we have two parallel helices on the same cylinder with the vorticity in the one just balancing that in the other."

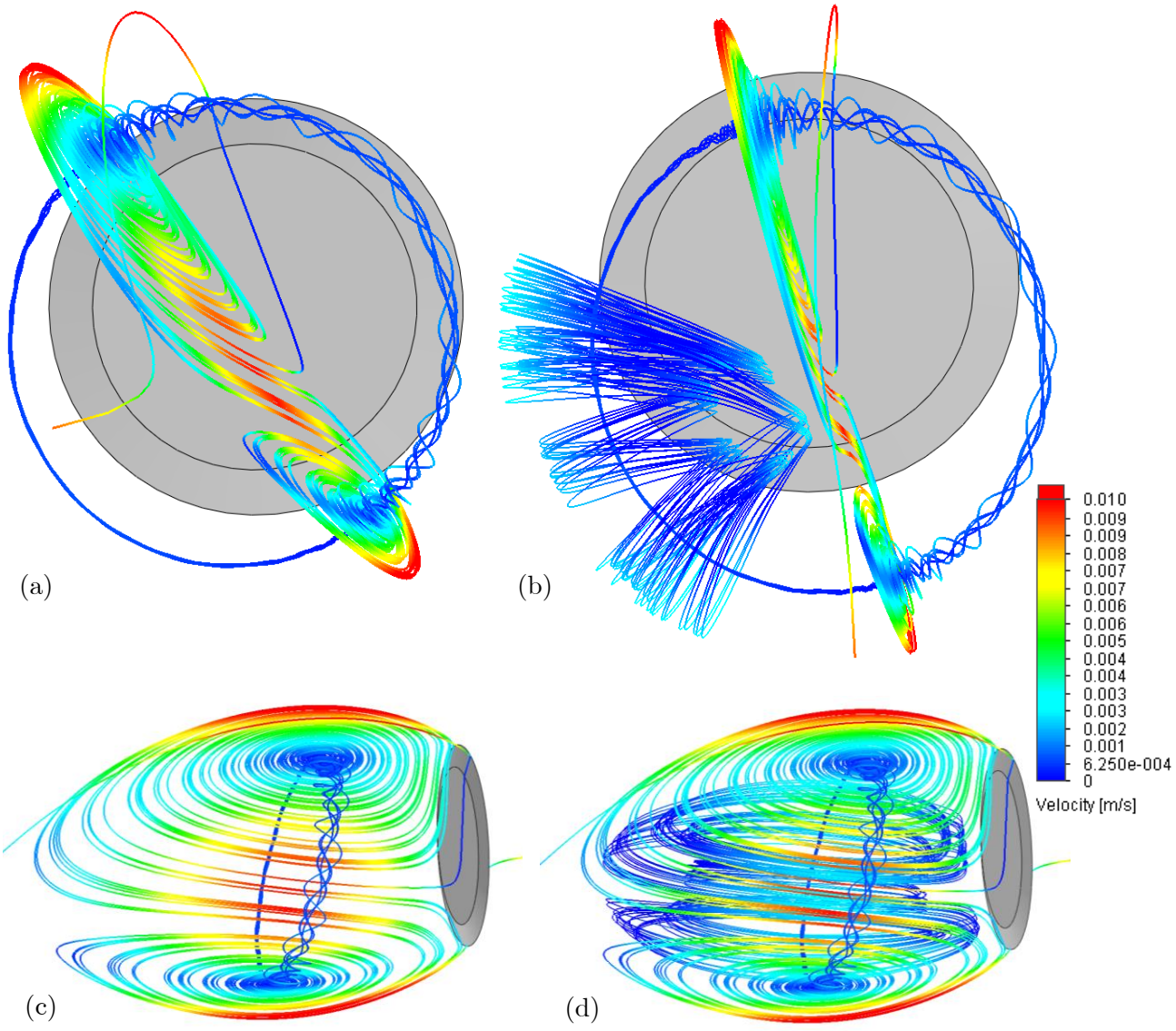

Figure 7. Wake behind a disk at $Re = 120$. (a) and (b): view from downstream looking upstream. In (a) and (c) a single streamline is shown. In (b) and (d), the same streamline is shown along with a second streamline which appears to never crosses the plane preferred by the first streamline. Number of computational cells: 619,366. $\nu = 1.338 \times 10^{-5}\,\mathrm{m}^2/\mathrm{s}$, $c_D = 1.25$.

4. Discussion

At least since the publication of the initial treatise by Syred and Beér (1974) on swirl-stabilized combustors, it has been known that swirl has a stabilizing effect on axisymmetric vortices. Since that time, interest in this topic has steadily increased (see, e.g., Pipitone & Mancuso 2005, Syred 2006, Stöhr *et al.* 2011). Today, the fact that swirl increases the stability of a vortex is relied upon heavily in the design of swirl-stabilized combustors (see, e.g., Palies *et al.* 2009, Lückoff *et al.* 2018). It is noteworthy that a steady vortex ring can be produced experimentally with a certain critical magnitude of swirl imparted during formation, but that unsteady oscillations are produced for swirl magnitudes greater or less

than this amount (Turkington 1989). The closest solution we have to the axisymmetric vortex in the wake bubble trailing normal disks is the spherical vortex of Hill (1894). Its velocity field and vorticity field have fore-aft symmetry; however, its pressure field does not. Therefore, this asymmetry is worthy of examination.

4.1 Hill's Spherical Vortex

1. Velocity Field

Hill's spherical vortex can be examined phenomena potentially associated with the loss in axisymmetry in the disk wake. To get the velocity field in Hill's spherical vortex, define components $\tilde{x}^i$ of a spherical coordinate system as follows:

$$\begin{aligned} x = x^1 &= \tilde{x}^1 \sin(\tilde{x}^2)\cos(\tilde{x}^3) \\ y = x^2 &= \tilde{x}^1 \sin(\tilde{x}^2)\sin(\tilde{x}^3) \\ z = x^3 &= \tilde{x}^1 \cos(\tilde{x}^2) \end{aligned}$$

Here, $\tilde{x}^1 = \sqrt{x^2 + y^2 + z^2} = r$, $\tilde{x}^2 = \theta$, and $\tilde{x}^3 = \phi$. The spherical coordinate system is shown in Figure 8.

From the transformation above, the metric tensor $\tilde{g}_{ij}$ relating the spherical coordinate system to a rectangular system is found to be

$$\tilde{g}_{ij} = \begin{bmatrix} 1 & 0 & 0 \\ 0 & r^2 & 0 \\ 0 & 0 & r^2 \sin^2\theta \end{bmatrix}.$$

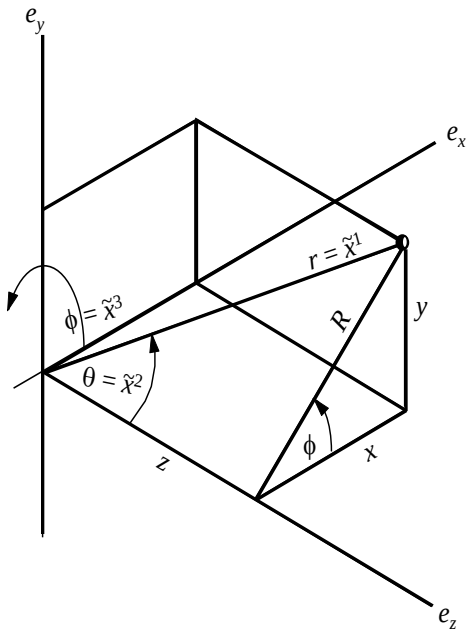

Figure 8. Spherical coordinate system used for Hill's spherical vortex.

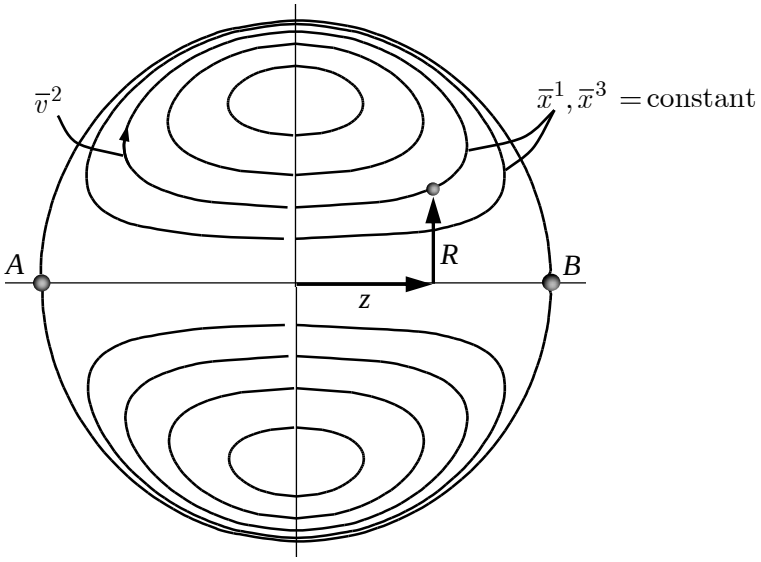

Figure 9. Streamlines of Hill's spherical vortex. Shown is any cross section through the sphere center containing the forward and rear stagnation points A and B, respectively.

Streamlines on a cross section of the core of Hill's spherical vortex are shown in Figure 9. The velocity tensor field inside Hill's spherical vortex is given in spherical coordinates by Morton (2004):

$$\tilde{v}^1 \;=\; v_H\!\left(1 \;-\; \frac{r^2}{{R_H}^2}\right)\cos\theta\,, \qquad \tilde{v}^2 \;=\; v_H\left(\frac{2r}{{R_H}^2} \;-\; \frac{1}{r}\right)\sin\theta\,, \qquad \tilde{v}^3 \;=\; 0\,, \tag{3}$$

where v_H is the maximum velocity on the perimeter of the sphere (where $r = R_H$).

If the velocity field in (3) is transformed to cylindrical coordinates (R,θ,z), defined by (see Morton 2016)

$$\begin{aligned} \hat{x}^1 &= z = r\cos\theta = \tilde{x}^1\cos(\tilde{x}^2) \\ \hat{x}^2 &= R = r\sin\theta = \tilde{x}^1\sin(\tilde{x}^2) \\ \hat{x}^3 &= \phi = \tilde{x}^3, \end{aligned} \tag{4}$$

then on any plane made by holding ϕ constant, the velocity field given in (3) becomes

$$\hat{v}^1 \;=\; v_H\left[1 - \left(\frac{z}{R_H}\right)^2 - 2\left(\frac{R}{R_H}\right)^2\right], \qquad \hat{v}^2 \;=\; v_H\,\frac{zR}{{R_H}^2}\,, \qquad \hat{v}^3 \;=\; 0\,. \tag{5}$$

This form will be more useful for examining streamwise effects.

2. Pressure Field

To examine the pressure field in the core of Hill's spherical vortex, the velocity field can be substituted into the momentum equation, which is then integrated. The momentum equation that is valid for compressible flow with constant viscosity is:

$$\frac{\partial \boldsymbol{v}}{\partial t} \;+\; \boldsymbol{v}\cdot\nabla\boldsymbol{v} \;=\; \boldsymbol{g} \;-\; \frac{1}{\rho}\nabla p \;+\; \nu\left[\nabla^2\boldsymbol{v} \;+\; \frac{1}{3}\nabla(\nabla\cdot\boldsymbol{v})\right], \tag{6}$$

Here, ν is the kinematic viscosity of the fluid, and ρ is the fluid density. Since Hill's spherical vortex is an incompressible flow, the last term in brackets is zero.

To find the pressure field in the core of the vortex, the velocity in (5) is substituted into (6), which is then integrated to find the pressure. The result is

$$\frac{\Delta p}{\rho {v_H}^2} = \frac{R^4}{2{R_H}^4} - \frac{R^2}{2{R_H}^2} + \frac{z^2}{{R_H}^2} - \frac{z^4}{2{R_H}^4} + \frac{1}{8} - 10\,\nu\frac{z}{v_H {R_H}^2}\,. \qquad (7)$$

Here, $\Delta p = (p - p_C)$ is the pressure difference between any point in the vortex and the pressure p_C at stationary points on the core circle (where $R = R_H/\sqrt{2}$, $z = 0$). The pressure distribution in (7) agrees with that reported by Llewellyn Smith and Ford (2001) for the core of their spherical vortex, with the exception of the viscous term since they employed the Euler equations. A surface plot of the pressure field in the spherical vortex is shown in Figure 10, revealing two pressure maxima at ($r = R_H/\sqrt{2}$, $\theta = 0, \pi$). It is imperceptible in the figure, but the pressure at point B does not quite return to the maximum at point A. This is because in (7), the viscous contribution to the pressure field contains the coordinate z, which is the streamwise distance from what would otherwise be a symmetry axis. Therefore, the effect of the viscous term is to break mirror symmetry about the y-axis. Since the pressure at B is lower than that at A, fore/aft symmetry is absent even in what looks like a symmetric flow. It only becomes apparent to the observer when the vortex loses its axisymmetry at Re_{C1}.

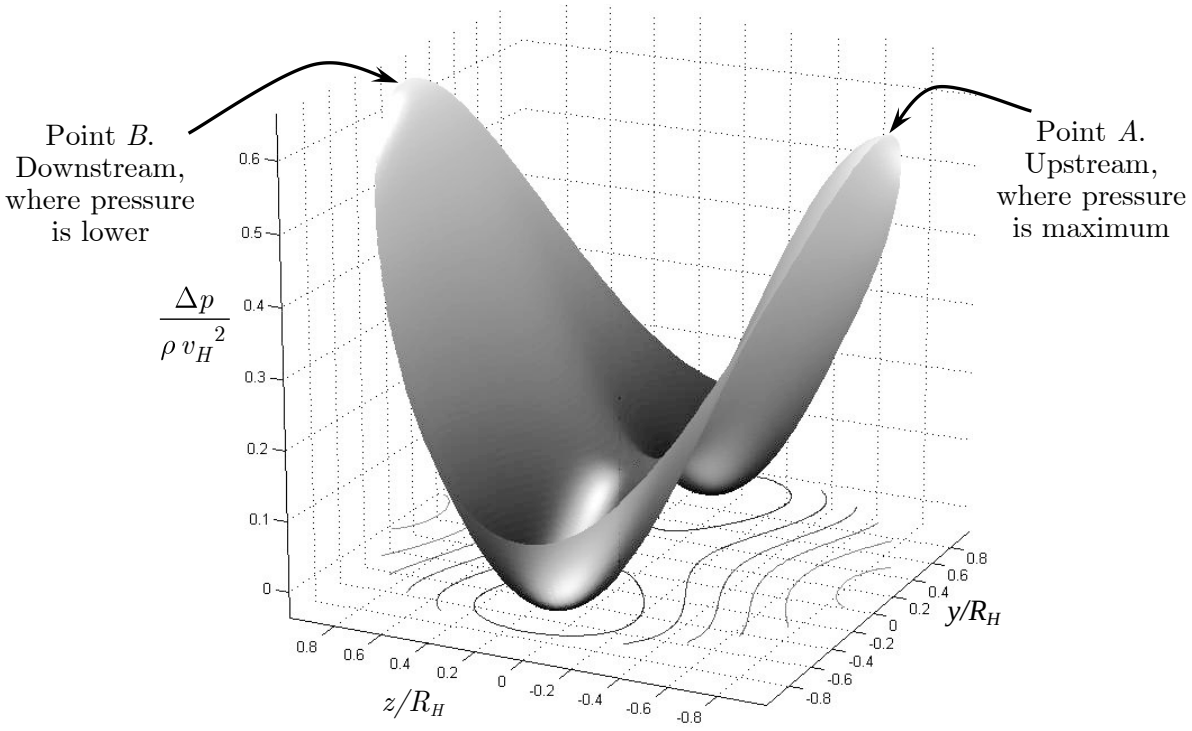

Figure 10. Surface plot of pressure field in Hill's spherical vortex. The surface for which the pressure is plotted is any cross section containing a closed streamline. Contours of pressure are shown projected onto the z-y plane. $\nu = 10^{-4}$.

3. Vorticity Field

In the spherical coordinate system, the vorticity tensor is uniform (see Morton 2004) and given by

$$\tilde{\omega}^1 = 0\,, \qquad \tilde{\omega}^2 = 0\,, \qquad \tilde{\omega}^3 = 5v_H/{R_H}^2\,, \tag{8}$$

and the physical vorticity is proportional to distance from the symmetry axis:

$$\tilde{\omega}(3)_{\text{Hill}} = \sqrt{\tilde{g}_{33}}\tilde{\omega}^3 = R\tilde{\omega}^3\,.$$

Note, therefore, that even though $\nu\nabla^2\boldsymbol{\omega} = 0$, it is not true that $\nu\nabla^2\boldsymbol{v} = 0$. Taking the curl of the momentum equation washes out some information about the viscous term in the resulting vorticity equation. So while Hill's spherical vortex is sometimes referred to in the literature as an inviscid solution, the core is actually a viscous flow. The viscous nature of the core of Hill's spherical vortex was first recognized by Hadamard (1911; see also O'Brien 1961).

The core of the spherical vortex is a flow in which the velocity, and hence the vorticity, has fore/aft symmetry, while the pressure field does not, as seen in (7). This asymmetric pressure field means that a fluid particle initially at a high pressure near the disk (close to p_A) sees pressure drop as it travels rearward until it passes the core circle, after which point it sees pressure begin to increase again. However, due to viscous effects, it does not attain the high pressure it saw near point A. Instead, it only attains a pressure close to p_B. (Recall that $p_A > p_B$). Now the question is: Having failed, near point B, to completely attain the pressure it had near point A, will it then be able to return back to the point near A and still fully recover the highest pressure in the loop, or will its pressure loss cause it to be diverted slightly along its path? The CFD runs above suggest the latter.

5. Conclusion

The wake structure behind a normal circular disk is investigated numerically. An interesting reversing helical vortex ring was found to exist for Reynolds numbers between 50 and 120, with nested stream surfaces resembling Reeb foliations. The fore/aft asymmetry in the pressure field may be a contributor to the streamline drift seen in these flows generally regarded as steady and axisymmetric.

References

Auguste, F., Fabre, D., & Magnaudet, J., "Bifurcations in the wake of a thick circular disk," *Theoretical and Computational Fluid Dynamics* **24** (2010) pp. 305-313.

Berger, E., Scholz, D., & Schumm, M., "Coherent vortex structures in the wake of a sphere and a circular disk at rest and under forced vibrations," *Journal of Fluids and Structures* **4** (1990) pp. 231-257.

Calvert, J. R., "Experiment on the flow past an inclined disk," *Journal of Fluid Mechanics* **29** (1967) pp. 691-703.

Camacho, C. & Neto, A. L., *Geometric Theory of Foliations*, Birkhäuser Boston (1984).

Candel, A. & Conlon, L., *Foliations I*, American Mathematical Society, Providence, Rhode Island (2000).

Fabre, D., Auguste, F., & Magnaudet, J., "Bifurcations and symmetry breaking in the wake of axisymmetric bodies," *Physics of Fluids* **20** (2008) pp. 051702-1-4.

Fernandes, P. C., Risso, F., Ern, P., & Magnaudet, J., "Oscillatory motion and wake instability of freely rising axisymmetric bodies," *Journal of Fluid Mechanics* **573** (2007) pp. 479-502.

Fuchs, H. V., Mercker, E., & Michel, U., "Large-scale coherent structures in the wake of axisymmetric bodies," *Journal of Fluid Mechanics* **93** (1979) pp. 185-207.

Hadamard, J., "Mouvement permanent lent d'une sphere liquide et visqueuse dans un liquide visqueux," *Comptes Rendus* **152** (1911) pp. 1735-1738.

Hill, M. J. M., "On a Spherical Vortex," *Philosophical Transactions of the Royal Society of London, A* **185** (1894) pp. 213-245.

Hwang, H. H. C. & Baldwin, L. V., "Decay of Turbulence in Axisymmetric Wakes," *ASME Journal of Basic Engineering, D* **88** (1966) pp. 261-268.

Jeffreys, H., "The Wake in Fluid Flow Past a Solid," *Proceedings of the Royal Society* (*London*) *A* **128** (1930) pp. 376-393.

Johnson, T. A. & Patel, V. C., "Flow past a sphere up to a Reynolds number of 300," *Journal of Fluid Mechanics* **378** (1999) pp. 19-70.

Lawson, Jr., H. B., "Foliations," *Bulletin of the American Mathematical Society* **80** (1974) pp. 369-418.

Lee, S. I. & Bearman, P. W., "An experimental investigation of the wake structure behind a disk," *Journal of Fluids and Structures* **6** (1992) pp. 437-450.

Levi, E., "A Universal Strouhal Law," *Journal of Engineering Mechanics, ASCE* **109** (1983) pp. 718-727.

Llewellyn Smith, S. G. & Ford, R., "Three-dimensional acoustic scattering by vortical flows. II. Axisymmetric scattering by Hill's spherical vortex," *Physics of Fluids* **13** (2001) pp. 2890-2900.

Lückoff, F., Sieber, M., Paschereit, C. O., & Oberleithner, K., "Characterization of Different Actuator Designs for the Control of the Precessing Vortex Core in a Swirl-Stabilized Combustor," Journal of Engineering for Gas Turbines and Power 140 (2018) pp. 041503-1-10.

Magarvey, R. H. & Bishop, R. L., "Transition ranges for three-dimensional wakes," *Canadian Journal of Physics* **39** (1961) pp. 1418-1422.

Marshall, D. & Stanton, T. E., "On the Eddy System in the Wake of Flat Circular Plates in Three Dimensional Flow, *Proceedings of the Royal Society of London A* **130** (1931) pp. 295-301 (17 pages including plates).

Miau, J. J., Leu, T. S., Liu, T. W., & Chou, J. H., "On vortex shedding behind a circular disk," *Experiments in Fluids* **23** (1997) pp. 225-233.

Mishra, P., Patel, S.A., Trivedi, M., & Chhabra, R.P., "Effect of Power-Law Fluid Behaviour on Nusselt Number of a Circular Disk in the Forced Convection Regime," *Journal of Heat Transfer* **141** (2019) pp. 041701-1-8.

Morton, T. S., "The velocity field within a vortex ring with a large elliptical cross-section," *J. Fluid Mech.* **503** (2004) pp. 247-271.

Morton, T. S., "A correlation between drag and an integral property of the wake vortex," arXiv.org:physics/0605209v3 (2007).

Morton, T. S., "A parameter for a family of steady vortex ring cores," *European Journal of Mechanics - B/Fluids* **56** (2016) pp. 66-70.

Natarajan, R. & Acrivos, A., "The instability of the steady flow past spheres and disks," *Journal of Fluid Mechanics* **254** (1993) pp. 323-344.

Nitin, S. & Chhabra, R.P., "Wall effects in two-dimensional axisymmetric flow over a circular disk oriented normal to flow in a cylindrical tube," *The Canadian Journal of Chemical Engineering* **83** (2005) pp. 450-457.

O'Brien, V., "Steady spheroidal vortices – More exact solutions to the Navier-Stokes equation," *Quarterly of Applied Mathematics* **19** (1961) pp. 163-168.

Palies, P., Durox, D., Schuller, T., Morenton, P., & Candel, S., "Dynamics of premixed confined swirling flames," *Comptes Rendus Mécanique* **337** (2009) pp. 395–405.

Pipitone, E. & Mancuso, U., "An experimental investigation of two different methods for swirl induction in a multivalve engine," *International Journal of Engine Research* **6** (2005) pp. 159-170.

Reeb, G., "Sur Certaines Propriétés Topologiques des Variétés Feuillétées" ("On Certain Topological Properties of Foliation Varieties"), *Actualités Scientifiques et Industrielles*, Hermann, Paris (1952).

Roberts, J. B., "Coherence Measurements in an Axisymmetric Wake," *AIAA Journal* **11** (1973) pp. 1569-1571.

Roos, F. W. & Willmarth, W. W., "Some Experimental Results on Sphere and Disk Drag," *AIAA Journal* **9** (1971) pp. 285-291.

Saha, A. K., "Three-dimensional numerical simulations of the transition of flow past a cube," *Physics of Fluids* **16** (2004) pp. 1630-1646.

Shenoy, A. R. & Kleinstreuer, C., "Flow over a thin circular disk at low to moderate Reynolds numbers," *Journal of Fluid Mechanics* **605** (2008) pp. 253-262.

Stanton, T. E. & Marshall, D., "Eddy systems behind discs," *Aeronautical Research Committee Reports and Memoranda*, No. 1358 (1932).

Stöhr, M., Boxx, I., Carter, C., & Meier, W., "Dynamics of lean blowout of a swirl-stabilized flame in a gas turbine model combustor," *Proceedings of the Combustion Institute* **33** (2011) pp. 2953-2960.

Syred N. & Beér, J. M., "Combustion in Swirling Flows: A Review," *Combustion and Flame* **23** (1974) pp. 143~201.

Syred, N., "A review of oscillation mechanisms and the role of the precessing vortex core (PVC) in swirl combustion systems," *Progress in Energy and Combustion Science* **32** (2006) pp. 93–161.

Tian, X., Ong., M. C., Yang, J., & Myrhaug, D., "Large-eddy simulations of flow normal to a circular disk at Re = 1.5×10^5," *Computers & Fluids* **140** (2016) pp. 422-434.

Turkington, B., "Vortex Rings with Swirl: Axisymmetric Solutions of the Euler Equations with Nonzero Helicity," *SIAM J. Math. Anal.* **20** (1989) pp. 57-73.

Willmarth, W. W., Hawk, N. E., & Harvey, R. L., "Steady and unsteady motions and wakes of freely falling disks," *Physics of Fluids* **7** (1964) pp. 197-208.

Yang, J., Wub, G., Zhong, W., & Liu, M., "Numerical study on bifurcations in the wake of a circular disk," *International Journal of Computational Fluid Dynamics* **28** (2014) pp. 187-203.